Trinuclear Angular Aggregates of Rhodium: Synthesis and Crystal Structures of $[Rh_3(\mu_3\text{-}SC_5H_4N)_2(CO)_6][ClO_4]$ (SC_5H_4N = pyridine-2-thiolate) and $[Rh_3(\mu_3\text{-}C_7H_4NS_2)_2(CO)_2(PPh_3)_2(tfbb)][ClO_4]$ ($C_7H_4NS_2$ = benzothiazole-2-thiolate, tfbb = tetrafluorobenzobarrelene) [*]

Miguel A. Ciriano, Jesús J. Perez-Torrente, Fernando Viguri, Fernando J. Lahoz, and Luis A. Oro
Departamento de Quimica Inorganica, Instituto de Ciencia de Materiales de Aragón, Universidad de Zaragoza-C.S.I.C., 50009 Zaragoza, Spain
Antonio Tiripicchio and Marisa Tiripicchio-Camellini
Istituto di Chimica Generale ed Inorganica, Università di Parma, Centro di Studio per la Strutturistica Diffrattometrica del CNR, Viale delle Scienze, 43100 Parma, Italy

The binuclear complexes $[\{Rh(\mu\text{-}L)L'_2\}_2]$ {L = pyridine-2-thiolate ($SC_5H_4N^-$) or benzothiazole-2-thiolate ($C_7H_4NS_2^-$); L'_2 = cyclo-octa-1,5-diene (cod), norborna-2,5-diene (nbd), tetrafluorobenzobarrelene (tetrafluorobenzo[5,6]bicyclo[2.2.2]octa-2,5,7-triene, tfbb), $(CO)_2$, or $(CO)(PPh_3)$} react with the appropriate species *cis*-$[RhL'_2(Me_2CO)_x]^+$ to give trinuclear aggregates $[Rh_3(\mu_3\text{-}L)_2(L'_2)_3][ClO_4]$. A study of this reaction has led to the controlled synthesis of a single isomer of the complexes $[Rh_3(\mu_3\text{-}C_7H_4NS_2)_2(CO)_2(PPh_3)_2L'_2][ClO_4]$. The trinuclear complexes have been characterized by ^1H, ^{31}P n.m.r., and u.v.-visible spectroscopy and in the case of $[Rh_3(\mu_3\text{-}SC_5H_4N)_2(CO)_6][ClO_4]\cdot 0.5CH_2Cl_2$ (**4**) and $[Rh_3(\mu_3\text{-}C_7H_4NS_2)_2(CO)_2(PPh_3)_2(tfbb)][ClO_4]$ (**12**) by single-crystal *X*-ray diffraction methods. In both structures trinuclear cationic rhodium complexes are present, in which two pyridine-2-thiolate[(**4**)] or benzothiazole-2-thiolate[(**12**)] ligands, acting as triple bridges through the nitrogen and one sulphur atom, interact with all three metal atoms, which are in a bent arrangement. Carbonyl ligands [(**4**)] and carbonyl, PPh_3, and tfbb (through the two double bonds) ligands [(**12**)] complete the slightly distorted square-planar co-ordination of the Rh atoms.

We have described the ability of small bite bidentate ligands having a N–C–S donor moiety, such as pyridine-2-thiolate ($SC_5H_4N^-$) and benzothiazole-2-thiolate ($C_7H_4NS_2^-$), to bridge metal atoms in rhodium[1–3] and iridium[4,5] complexes through either the sulphur atom or both N and S ends. In the latter co-ordination mode, they behave similarly to ligands having a N–C–X (X = N or O) donor moiety which bring the metal atoms in close proximity. A mutually *cis* disposition of these small-bite ligands is generally adopted in binuclear complexes. Representative examples are $[\{Rh(\mu\text{-}L)(nbd)\}_2]$[6] (L = 1*H*-pyrrolo[2,3-*b*]pyridinate, nbd = norborna-2,5-diene), $[\{Rh(\mu\text{-}Onapy)(CO)_2\}_2]$[7a] (Onapy = 1,8-naphthyridine-2-onate), $[Rh_3(\mu_3\text{-}Onapy)_2(cod)_2(CO)_2][ClO_4]$[7b] (cod = cyclo-octa-1,5-diene), and $[\{Rh(\mu\text{-}Opy)(CO)_2\}_2]$[8] (Opy = 2-pyridonate). Another unusual feature of the N–C–S ligands, related probably to the disposition of the bridges and the association of a soft and hard donor atom, is the stabilization of unusual compounds such as the first tetrairidium linear chain$[Ir_4(\mu\text{-}C_7H_4NS_2)_4I_2(CO)_8]$.[5] In addition, these ligands can bridge two metals through the sulphur atom only, so allowing the nitrogen atom to bind a third metal centre. In this way, the N–C–S ligands, being five-electron donors, might lead to the controlled synthesis of aggregates.[9]

Herein we describe in full the preparation, structure, and the mode of formation of trinuclear complexes of rhodium with the pyridine-2-thiolate and benzothiazole-2-thiolate ligands. Part of these results has been subject of preliminary communications.[1,2]

Results and Discussion

Deep green solutions of trinuclear complexes $[Rh_3(\mu_3\text{-}SC_5H_4N)_2(diolefin)_3]^+$ are readily formed by reaction of $[\{Rh(\mu\text{-}SC_5H_4N)(diolefin)\}_2]$ and $[\{Rh(\mu\text{-}Cl)(diolefin)\}_2]$ in a polar donor solvent such as methanol or acetone. No reaction takes place in a non-co-ordinating solvent such as dichloromethane, so that the solvent plays a basic role in providing rhodium cationic species. Further addition of a poorly co-ordinating anion (ClO_4^-) allows the isolation of the crude compounds $[Rh_3(\mu_3\text{-}SC_5H_4N)_2(diolefin)_3][ClO_4]$ {diolefin = cod, (**1**), nbd, (**2**); or tetrafluorobenzobarrelene (tetrafluorobenzo[5,6]-bicyclo[2.2.2]octa-2,5,7-triene, tfbb), (**3**)} in moderate yields. A rational straightforward and high-yield synthesis for compounds (**1**)—(**3**) is accomplished by addition of $[Rh(diolefin)(Me_2CO)_x]^+$ to the appropriate binuclear complex $[\{Rh(\mu\text{-}SC_5H_4N)(diolefin)\}_2]$ in acetone. Interestingly, solutions of complex (**1**) are dichroic (red by transmitted and green by reflected light). Complexes (**1**)—(**3**) show bands due to anionic perchlorate (T_d) in their i.r. spectra in the solid state and behave as 1:1 electrolytes in solution (see Table 1) in acccordance with the proposed formulation.

Carbon monoxide at atmospheric pressure replaces the diolefin in complexes (**1**)—(**3**) to give the trinuclear complex $[Rh_3(\mu_3\text{-}SC_5H_4N)_2(CO)_6][ClO_4]$ (**4**) which should be crystallized under an atmosphere of carbon monoxide, otherwise the reaction is reversed.

Although analytical and spectroscopic data for complexes (**1**)—(**4**) (Table 1) are consistent with trinuclear cationic complexes, the structure of one of these, (**4**), was unequivocally

---

[*] Bis(μ_3-pyridine-2-thiolato-*N*,μ-*S*)-tris(dicarbonylrhodium)perchlorate and bis(μ_3-benzothiazole-2-thiolato-*N*,μ-*S*)-1,3-dicarbonyl-2-{tetrafluorobenzo[5,6]bicyclo[2.2.2]octa-2,5,7-triene-$C^{2,3,5,6}(Rh^2)$}-1,3-bis(triphenylphosphine)trirhodium perchlorate.

Supplementary data available: see Instructions for Authors, *J. Chem. Soc., Dalton Trans.*, 1990, Issue 1, pp. xix—xxii.

Table 1. Analytical and physical properties of the new complexes

Compound	Colour	Yield (%)	Analysis (%)^a C	H	N	Λ_M^{b}	ν(CO)^c/cm^{-1}
(**1**) $[Rh_3(\mu_3\text{-}SC_5H_4N)_2(cod)_3][ClO_4]$	Green	89	42.9 (42.85)	4.6 (4.65)	3.1 (2.95)	85	
(**2**) $[Rh_3(\mu_3\text{-}SC_5H_4N)_2(nbd)_3][ClO_4]$	Green	74	41.4 (41.15)	3.6 (3.75)	3.0 (3.10)	95	
(**3**) $[Rh_3(\mu_3\text{-}SC_5H_4N)_2(tfbb)_3][ClO_4]$	Green	76	41.8 (42.25)	2.0 (2.00)	2.4 (2.15)	120	
(**4**) $[Rh_3(\mu_3\text{-}SC_5H_4N)_2(CO)_6][ClO_4]$	Purple	82	25.7 (26.10)	1.4 (1.10)	4.0 (3.80)	107	2 100s, 2 080s, 2 035s, 2 020 (sh), 2 000 (sh)
(**5**) $[Rh_3(\mu_3\text{-}C_7H_4NS_2)_2(cod)_3][ClO_4]$	Green-grey	85	42.8 (42.90)	3.9 (4.1)	2.6 (2.60)	130	
(**6**) $[Rh_3(\mu_3\text{-}C_7H_4NS_2)_2(nbd)_3][ClO_4]$	Dark green	85	41.6 (41.35)	3.3 (3.15)	2.8 (2.75)	136	
(**7**) $[Rh_3(\mu_3\text{-}C_7H_4NS_2)_2(tfbb)_3][ClO_4]$	Green	88	42.2 (42.30)	1.8 (1.85)	1.8 (1.95)	122	
(**8**) $[Rh_3(\mu_3\text{-}C_7H_4NS_2)_2(CO)_6][ClO_4]$	Violet	79	27.2 (26.45)	1.2 (0.90)	3.1 (3.10)	148	2 088vs, 2 055s, 2 020vs
(**9**) $[Rh_3(\mu_3\text{-}C_7H_4NS_2)_2(CO)_3(PPh_3)_3][ClO_4]$	Dark red	90	52.5 (52.90)	3.4 (3.30)	1.6 (1.75)	106	2 000vs
(**10**) $[Rh_3(\mu_3\text{-}C_7H_4NS_2)_2(CO)_2(PPh_3)_2(cod)][ClO_4]$	Dark blue	94	49.6 (50.40)	3.4 (3.50)	1.8 (1.95)	138	1 995vs
(**11**) $[Rh_3(\mu_3\text{-}C_7H_4NS_2)_2(CO)_2(PPh_3)_2(nbd)][ClO_4]$	Violet	87	50.4 (50.15)	3.1 (3.30)	2.0 (2.00)	131	1 992vs
(**12**) $[Rh_3(\mu_3\text{-}C_7H_4NS_2)_2(CO)_2(PPh_3)_2(tfbb)][ClO_4]$	Green	90	49.4 (49.65)	3.1 (2.70)	1.5 (1.80)	118	1 996vs
(**13**) $[Rh_3(\mu_3\text{-}C_7H_4NS_2)_2(CO)_4(PPh_3)_2][ClO_4]$	Violet	82	46.7 (47.10)	2.9 (2.80)	2.2 (2.05)	131	2 085s, 2 040s, 2 020s
(**14**) $[Rh_3(\mu_3\text{-}C_7H_4NS_2)_2(CO)_2(tfbb)_2][ClO_4]$	Green	92	38.4 (38.45)	1.6 (1.60)	2.4 (2.25)	129	2 085vs, 2 038s

^{a} Calculated values are given in parentheses. ^{b} In acetone. ^{c} In CH_2Cl_2.

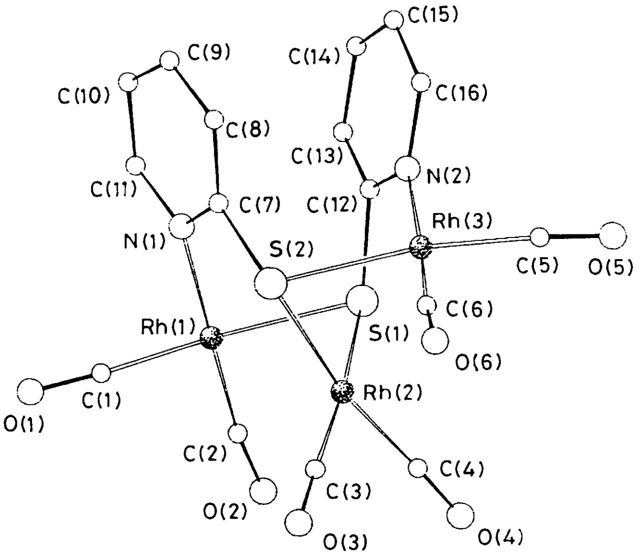

Figure 1. View of the cationic complex $[Rh_3(\mu_3\text{-}SC_5H_4N)_2(CO)_6]^+$ (**4**) with the atomic numbering scheme

determined by *X*-ray diffraction methods. Suitable crystals were grown by vapour diffusion of diethyl ether into a solution of complex (**4**) in dichloromethane.

Description of the Crystal Structure of $[Rh_3(\mu_3\text{-}SC_5H_4N)_2(CO)_6][ClO_4]\cdot 0.5CH_2Cl_2$ (**4**).—In the unit cell of complex (**4**) two crystallographically independent but essentially identical cations $[Rh_3(\mu_3\text{-}SC_5H_4N)_2(CO)_6]^+$ are present along with two ClO_4^- anions and one CH_2Cl_2 molecule of solvation. The structure of one of the two independent cations is depicted in Figure 1 together with the atomic numbering scheme; selected bond distances and angles are listed in Table 2. The Rh atoms are in a bent arrangement with Rh(1)–Rh(2)–Rh(3) 112.4(2) [112.7(2)]°; (all values in square brackets refer to the second independent cation) and the two pyridine-2-thiolate ligands interact with all three metals. The Rh(1) ··· Rh(2) and Rh(2) ··· Rh(3) separations, 2.891(5) [2.927(5)] and 2.907(4) [2.920(4)] Å, are indicative of weak metal–metal interactions. Each ligand is bound to one metal through the nitrogen atom and to the other two through the sulphur atom. Each Rh atom completes its co-ordination with two terminal carbonyl groups and is in a slightly distorted, but different, square-planar arrangement. The central metal, Rh(2), is bonded also to two thiolate sulphur atoms, whereas the terminal ones are bonded to one nitrogen and one sulphur atom from two pyridine-2-thiolate ligands. The co-ordination around Rh(2) is more distorted than those around the terminal Rh atoms, probably because of the constraints of the bridging sulphur atoms, {deviations from mean planes: through C(3), C(4), S(1), and S(2), C(3) 0.37(2) [0.26(2)], C(4) −0.40(3) [−0.36(2)], S(1) 0.013(5) [0.012(5)], S(2) −0.013(5) [−0.012(5)], and Rh(2) 0.016(4) [0.008(5)] Å; through C(1), C(2), N(1), and S(1), C(1) 0.16(2) [0.10(2)], C(2) −0.15(2) [−0.09(2)], N(1) −0.04(1) [−0.03(1)], S(1) 0.006(5) [0.003(5)], and Rh(1) −0.074(5) [−0.033(4)] Å; through C(5), C(6), N(2), and S(2), C(5) 0.06(2) [0.17(2)], C(6) −0.06(3) [−0.24(3)], N(2) −0.02(1) [−0.05(1)], S(2) 0.002(5) [0.007(5)], and Rh(3) −0.018(4) [−0.059(3)] Å}. The reciprocal disposition of the co-ordination planes around Rh(1) and Rh(3) with respect to that around Rh(2) is indicated by the dihedral angles of 71.9(4) [74.2(4)] and 72.8(4) [73.3(4)]° respectively.

The pyridine-2-thiolate ligands are perfectly planar except for

Table 2. Selected bond distances (Å) and angles (°) for complex (**4**)

	Molecule 1	Molecule 2		Molecule 1	Molecule 2
Rh(1) ··· Rh(2)	2.891(5)	2.927(5)	N(1)–C(11)	1.37(2)	1.37(2)
Rh(2) ··· Rh(3)	2.907(4)	2.920(4)	C(7)–C(8)	1.41(3)	1.41(3)
Rh(1)–N(1)	2.106(13)	2.080(14)	C(8)–C(9)	1.39(3)	1.41(2)
Rh(1)–S(1)	2.407(6)	2.401(5)	C(9)–C(10)	1.38(3)	1.34(3)
Rh(1)–C(1)	1.81(3)	1.80(2)	C(10)–C(11)	1.34(3)	1.38(3)
Rh(1)–C(2)	1.83(2)	1.82(2)	N(2)–C(12)	1.34(2)	1.34(2)
Rh(2)–S(1)	2.366(5)	2.365(5)	N(2)–C(16)	1.35(2)	1.38(2)
Rh(2)–S(2)	2.388(6)	2.378(5)	C(12)–C(13)	1.40(3)	1.38(2)
Rh(2)–C(3)	1.86(2)	1.83(2)	C(13)–C(14)	1.41(3)	1.38(3)
Rh(2)–C(4)	1.87(3)	1.83(3)	C(14)–C(15)	1.39(3)	1.44(3)
Rh(3)–N(2)	2.085(14)	2.088(13)	C(15)–C(16)	1.44(3)	1.38(2)
Rh(3)–S(2)	2.417(6)	2.398(5)	C(1)–O(1)	1.12(3)	1.15(3)
Rh(3)–C(5)	1.80(3)	1.85(2)	C(2)–O(2)	1.15(3)	1.18(3)
Rh(3)–C(6)	1.78(2)	1.77(3)	C(3)–O(3)	1.13(3)	1.17(3)
S(1)–C(12)	1.769(18)	1.795(16)	C(4)–O(4)	1.15(4)	1.14(3)
S(2)–C(7)	1.770(17)	1.798(17)	C(5)–O(5)	1.15(3)	1.13(3)
N(1)–C(7)	1.34(2)	1.33(2)	C(6)–O(6)	1.19(3)	1.14(3)
S(1)–Rh(1)–N(1)	89.9(4)	89.6(4)	Rh(2)–S(2)–Rh(3)	74.5(2)	75.4(2)
N(1)–Rh(1)–C(1)	89.9(9)	91.7(9)	C(7)–S(2)–Rh(2)	114.0(6)	113.4(6)
C(1)–Rh(1)–C(2)	88.9(11)	89.0(11)	C(7)–S(2)–Rh(3)	107.7(6)	107.1(6)
S(1)–Rh(1)–C(2)	91.6(8)	89.8(8)	Rh(3)–N(2)–C(16)	114.7(12)	115.4(11)
S(1)–Rh(2)–S(2)	94.3(2)	93.3(2)	Rh(3)–N(2)–C(12)	123.9(12)	126.6(11)
S(2)–Rh(2)–C(3)	89.5(8)	89.0(7)	N(2)–C(12)–C(13)	122.3(16)	125.1(15)
C(3)–Rh(2)–C(4)	91.1(11)	91.1(11)	N(2)–C(12)–S(1)	121.0(13)	118.2(12)
S(1)–Rh(2)–C(4)	87.8(8)	88.3(9)	C(13)–C(12)–S(1)	116.7(14)	116.4(13)
S(2)–Rh(3)–N(2)	89.4(4)	90.0(4)	Rh(1)–S(1)–Rh(2)	74.6(2)	75.8(2)
N(2)–Rh(3)–C(5)	92.0(9)	93.0(8)	C(12)–S(1)–Rh(1)	107.1(6)	107.9(6)
C(5)–Rh(3)–C(6)	90.2(11)	89.8(11)	C(12)–S(1)–Rh(2)	113.7(6)	113.7(6)
S(2)–Rh(3)–C(6)	88.4(9)	88.0(9)	Rh(1)–C(1)–O(1)	173(2)	177(2)
Rh(1)–N(1)–C(7)	123.3(11)	124.7(11)	Rh(1)–C(2)–O(2)	174(2)	173(2)
Rh(1)–N(1)–C(11)	115.1(12)	116.2(11)	Rh(2)–C(3)–O(3)	176(2)	175(2)
N(1)–C(7)–C(8)	121.3(16)	124.0(16)	Rh(2)–C(4)–O(4)	170(2)	176(2)
N(1)–C(7)–S(2)	121.1(13)	119.2(13)	Rh(3)–C(5)–O(5)	177(2)	176(2)
S(2)–C(7)–C(8)	117.5(13)	116.7(13)	Rh(3)–C(6)–O(6)	175(2)	176(2)

the sulphur atoms which deviate from the mean planes through the pyridine rings by 0.097(6) [0.157(5)] for S(2) and 0.054(6) [0.171(5)] Å for S(1).

The Rh–S and Rh–N bonds, in the ranges 2.365(5)—2.417(6) and 2.080(14)—2.106(13) Å respectively, can be compared to those found in the binuclear complexes $[\{Rh(\mu\text{-}SC_5H_4N)(tfbb)\}_2]$, 2.320(2) and 2.112(6) Å (one pyridine-2-thiolate bridges through the sulphur only), and $[\{Rh(\mu\text{-}SC_5H_4N)(CO)_2\}_2]$, 2.364(2) and 2.118(6) Å, with the same ligand acting as a simple bridge through the N and S atoms.[3] Also the S ··· N bite of this ligand does not seem to be influenced by the different co-ordination behaviour, 2.714(14) [2.710(14)] and 2.715(15) [2.696(14)] Å in (**4**) and 2.636(6) and 2.692(7) Å in the binuclear complexes.

Complexes (**1**)—(**3**) should have the same framework as (**4**) but their ^1H n.m.r. spectra consist of broad resonances giving scarce structural information. In order to obtain a deeper insight into the generation of trinuclear complexes and to extract more information from spectroscopic studies, complexes with the bulky benzothiazole-2-thiolate ligand were prepared.

The complexes $[Rh_3(\mu_3\text{-}C_7H_4NS_2)_2(diolefin)_3][ClO_4]$[diolefin = cod, (**5**); nbd, (**6**); or tfbb, (**7**)] are formed immediately on addition of the solvated species $[Rh(diolefin)(Me_2CO)_x]^+$ to the appropriate $[\{Rh(\mu\text{-}C_7H_4NS_2)_2(diolefin)\}_2]$ complex, and were isolated from the deeply coloured solutions as air-stable microcrystalline solids in good yields. Bubbling of carbon monoxide through solutions of these complexes in dichloromethane gives a red-wine solution of $[Rh_3(\mu_3\text{-}C_7H_4NS_2)_2(CO)_6][ClO_4]$ (**8**), which should be isolated under an atmosphere of carbon monoxide to prevent the reverse reaction. As expected, complex (**8**) can also be prepared in high yield by addition of $[Rh(CO)_2(Me_2CO)_x]^+$ to a solution of $[\{Rh(\mu\text{-}C_7H_4NS_2)_2(CO)_2\}_2]$ in acetone. It reacts cleanly with triphenylphosphine, in contrast with complex (**4**), with evolution of carbon monoxide, to give the compound $[Rh_3(\mu_3\text{-}C_7H_4NS_2)_2(CO)_3(PPh_3)_3]$ $[ClO_4]$ (**9**). One carbonyl group remains co-ordinated to each rhodium atom giving rise to a broad ν(CO) band containing three i.r.-active modes. A single isomer is obtained in this reaction according to the $^{31}P\text{-}\{^1H\}$ n.m.r. spectrum.

Characterization and Structure of Complexes (**5**)—(**9**).—Complexes (**5**)—(**9**) show bands due to unco-ordinated perchlorate at 1 100 and 625 cm^{-1} in their i.r. spectra in the solid state. Accordingly their molar conductivities in acetone have values characteristic of 1:1 electrolytes (see Table 1).

The spectroscopic data for these compounds and those described below are consistent with structures having a basic '$Rh_3(\mu\text{-}S\text{–}C\text{–}N)_2$' framework similar to that of complex (**4**), Figure 2(*a*). The heterocyclic sulphur atom is not used for co-ordination and the ancillary ligands occupy the two positions remaining on each rhodium centre in a square-planar disposition. Thus, the ^1H n.m.r. spectra of the diolefin complexes (**5**)—(**7**) (see Table 3 and Figure 3) display sharp resonances invariant with temperature, in contrast with the parent binuclear complexes $[\{Rh(\mu\text{-}C_7H_4NS_2)(diolefin)\}_2]$. This lack of fluxional behaviour is probably imposed by the immobilization of the lone pairs of the exocyclic sulphur atoms upon co-ordination to the third metal centre. As exemplified in Figure 3, the benzothiazole-2-thiolate ligands are equivalent

Table 3. Proton and ^{31}P-{^{1}H} n.m.r. data for the new complexes[a]

Compound	^{1}H (δ)[b]	^{31}P (δ)[c]
(5)	8.49 (d, 2 H, H^4), 7.32 (dd of d, 2 H, H^5 or H^6), 7.05 (d of d, 2 H, H^7), 6.92 (dd of d, 2 H, H^5 or H^6), 5.67 (m, 2 H, =CH of cod), 5.46 (m, 2 H, =CH of cod), 4.70 (m, 2 H, =CH of cod), 4.30 (m, 2 H, =CH of cod), 3.7 (m, 4 H, =CH of cod), 3.4—2.9 (m, 6 H, CH_2 of cod), 2.7—2.0 (m, 12 H, CH_2 of cod), 1.9—1.5 (m, 6 H, CH_2 of cod)	
(6)	8.73 (d, 2 H, H^4), 7.34 (dd of d, 2 H, H^5 or H^6), 6.90 (m, 4 H, H^5 or H^6 and H^7), 5.21 (m, 4 H), 5.02 (m, 2 H), 4.50 (m, 2 H), 4.37 (m, 4 H), 4.21 (m, 2 H), 4.05 (m, 2 H), 3.91 (m, 2 H, =CH and CH of nbd), 1.70 (m, 2 H, CH_2 of nbd), 1.60 (m, 2 H, CH_2 of nbd), 1.40 (m, 2 H, CH_2 of nbd)	
(7)	9.18 (d, 2 H, H^4), 7.55 (dd of d, 2 H, H^5 or H^6), 7.31 (d of d, 2 H, H^7), 7.12 (dd of d, 2 H, H^5 or H^6), 6.65 (m, 4 H, CH of tfbb), 6.42 (m, 2 H, CH of tfbb), 5.81 (m, 2 H, =CH of tfbb), 5.15 (m, 4 H, =CH of tfbb), 4.72 (m, 2 H, =CH of tfbb), 4.52 (m, 2 H, =CH of tfbb), 4.10 (m, 2 H, =CH of tfbb)	
(9)		41.1 (d, 175), 39.4 (d, 168), 39.1 (d, 160)
(10)	7.85 (d, 2 H, H^4), 7.52 (m, 12 H, PPh_3), 7.31 (m, 18 H, PPh_3), 6.87 (dd of d, 2 H, H^5 or H^6), 6.71 (dd of d, 2 H, H^5 or H^6), 6.6 (d of d, 2 H, H^7), 4.83 (m, 2 H, =CH of cod), 4.02 (m, 2 H, =CH of cod), 2.37 (m, 2 H, CH_2 of cod), 1.65 (m, 6 H, CH_2 of cod)	41.6 (d, 167)
(11)	7.81 (d, 2 H, H^4), 7.52 (m, 12 H, PPh_3), 7.31 (m, 18 H, PPh_3), 6.94 (dd of d, 2 H, H^5 or H^6), 6.73 (dd of d, 2 H, H^5 or H^6), 6.62 (d of d, 2 H, H^7), 4.32 (m, 2 H, nbd), 4.17 (m, 2 H, nbd), 4.07 (m, 2 H, nbd), 1.67 (m, 2 H, CH_2 of nbd)	42.9 (d, 168)
(12)	7.93 (d, 2 H, H^4), 7.61 (m, 12 H, PPh_3), 7.37 (m, 18 H, PPh_3), 6.92 (dd of d, 2 H, H^5 or H^6), 6.7 (dd of d, 2 H, H^5 or H^6), 6.6 (d of d, 2 H, H^7), 5.1 (m, 2 H, CH of tfbb), 3.9 (m, 2 H, =CH of tfbb), 3.7 (m, 2 H, =CH of tfbb)	42.5 (d, 166)
(13)	7.95 (d, 2 H, H^4), 7.55 (m, 12 H, PPh_3), 7.30 (m, 18 H, PPh_3), 7.11 (dd of d, 2 H, H^5 or H^6), 6.95 (dd of d, 2 H, H^5 or H^6), 6.87 (d of d, 2 H, H^7)	40.6 (d, 169)
(14)	8.87 (d, 1 H, H^4), 8.17 (d, 1 H, H^4), 7.63 (m, 1 H, H^5 or H^6), 7.34 (m, 1 H, H^5 or H^6), 7.17 (m, 4 H, H^7 and H^5 or H^6), 6.3—6.0 (m, 3 H, CH of tfbb), 5.86 (m, 1 H, CH of tfbb), 5.31 (m, 1 H, =CH of tfbb), 5.19 (m, 1 H, =CH of tfbb), 4.83 (m, 2 H, =CH of tfbb), 4.36 (m, 2 H, =CH of tfbb), 4.06 (m, 2 H, =CH of tfbb)	

[a] In $CDCl_3$ at 20 °C. [b] The protons of the heterocyclic ligand are numbered according to the I.U.P.A.C. rules, starting from the heterocyclic sulphur. [c] Coupling constants ^{1}J(P–Rh) in parentheses (in Hz).

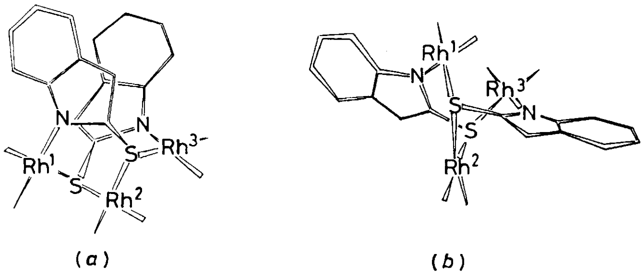

(a) (b)

Figure 2. Idealized drawings of the possible conformations of the framework '$Rh_3(\mu_3$-S–C–N$)_2$.' Each conformation has an enantiomer, which is not shown

in complexes (5)—(7) since they are related by a C_2 symmetry axis containing the Rh(2) atom in Figure 2. They give rise to four resonances in the δ 9.1—6.9 region. Interestingly, the deshielding of one of the protons of the fused benzene ring is due to the proximity of this proton to one metal centre and with the mode of co-ordination of the ligand as a bridge through the N and S atoms. The C_2 axis in (5)—(7) also groups the olefinic protons in six sets of equivalent nuclei, giving rise to six resonances between δ 5.8—3.7 of relative intensity 2:2:2:2:2:2.

Although derived from the same basic framework, in the structure of complex (9) neither the bridging nor the phosphine ligands are equivalent. Each phosphine ligand is bonded to a rhodium atom and gives rise to a doublet in the ^{31}P-{^{1}H} n.m.r. spectrum due to coupling with ^{103}Rh. For the terminal metals these phosphine ligands are *trans* to the sulphur atoms which have higher *trans* influence than the nitrogen, as can be observed by comparison of the Rh–C distances *trans* to S and N in the complex [{Rh(μ-SC_5H_4N)$(CO)_2$}$_2$].[3] Furthermore, phosphorus-donor ligands replace the carbonyl groups *trans* to sulphur in the complex [{Rh(μ-$C_3H_4NS_2$)$(CO)_2$}$_2$][10] ($C_3H_4NS_2$ = 2-mercapto-1,3-thiazolinate). In this way, two of the doublets have very similar chemical shifts since the chemical environments of atoms Rh(1) and Rh(3) are identical and the whole trinuclear complex lacks elements of symmetry.

The aforementioned ^{1}H and ^{31}P n.m.r. data would also be compatible with a structure derived from the open framework represented in Figure 2(*b*) but this is ruled out in view of the electronic spectra of complexes (5)—(9). Molecular models show that in Figure 2(*b*) two metal atoms, Rh(1) and Rh(3), might be in close proximity at metal–metal distances like those in the binuclear complex [{Rh(μ-SC_5H_4N)$(CO)_2$}$_2$]. The third metal atom, Rh(2), is far away from the others in the known structure[11] derived from this conformation of the eight-membered ring 'Rh_2(μ-N–C–S$)_2$'. In the structure in Figure 2(*a*), derived from the 'tub' conformation of the eight-membered ring 'Rh_2(μ-N–C–S$)_2$,' the three metal atoms are in a bent arrangement at distances of interaction between the two terminal ones and the central Rh(2). Furthermore, the d_{z^2} and p_z orbitals of the three metals, perpendicular to the co-ordination planes, can interact, whilst this interaction can occur only between the terminal metal atoms, Rh(1) and Rh(3), in structure (*b*). Complexes having a framework like that in Figure 2(*b*) should have electronic spectra similar to those of the related binuclear complexes [{Rh(μ-$C_7H_4NS_2$)L_2}$_2$] [see Table 4 and Figure 4(*a*)], *i.e.* one intense band in the visible region between 450 and 500 nm. This, so-called, 'proximity shift band,' observed for other compounds containing a d^8—d^8 chromophore, has been ascribed to metal–metal interactions either in face-to-face or open-book structures.[12–14] Perturbation of the out-of-plane orbitals (the filled d_{z^2} and the empty p_z) of each rhodium leads

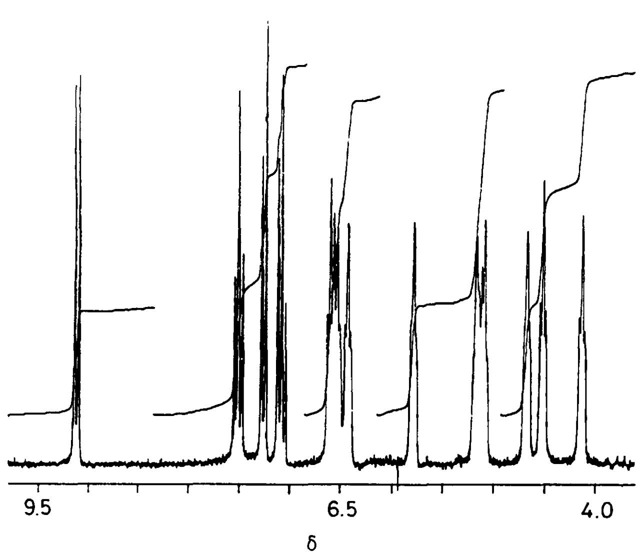

Figure 3. Proton n.m.r. spectrum of complex (**7**)

Table 4. Visible–u.v. spectra of bi- and tri-nuclear complexes *

Compound	$\lambda_{max.}$ (nm)
(**5**)	575 (3.9×10^3), 440 (5.1×10^3), 328 (2.1×10^4)
(**6**)	647 (4.8×10^3), 480 (3.8×10^3), 416 (5.0×10^3)
(**7**)	618 (4.5×10^3), 452 (4.6×10^3), 328 (3.7×10^4)
(**8**)	568 (3.3×10^3), 413 (5.4×10^3)
(**9**)	548 (6.4×10^3), 422 (6.8×10^3)
(**10**)	567 (5.8×10^3), 408 (6.5×10^3)
(**11**)	578 (7.4×10^3), 410 (6.4×10^3)
(**12**)	580 (6.8×10^3), 415 (7.2×10^3)
(**13**)	547 (7.1×10^3), 414 (5.8×10^3)
(**14**)	594 (4.5×10^3), 433 (5.8×10^3)
$[Rh(\mu\text{-}C_7H_4NS_2)(cod)]_2$	450 (1.2×10^3), 345 (1.4×10^4)
$[Rh(\mu\text{-}C_7H_4NS_2)(nbd)]_2$	493 (1.8×10^3), 410 (5.1×10^3), 328 (1.7×10^4)
$[Rh(\mu\text{-}C_7H_4NS_2)(tfbb)]_2$	445 (3.0×10^3)
$[Rh(\mu\text{-}C_7H_4NS_2)(CO)]_2$	485 (4.7×10^3)
$[Rh(\mu\text{-}C_7H_4NS_2)(CO)(PPh_3)]_2$	460 (2.2×10^3), 357 (2.0×10^4)

* Molar absorption coefficients (ε $dm^3\ mol^{-1}\ cm^{-1}$) in parentheses.

to a set of molecular orbitals in which the gap between the highest occupied and lowest unoccupied molecular orbitals (h.o.m.o. and l.u.m.o.) becomes smaller than in mononuclear complexes,[15,16] so that the allowed band $d_{\sigma^*} \longrightarrow p_\sigma$ falls in the visible region. As the number of metal atoms interacting in the aggregate increases, the shift to lower energies of the proximity band becomes larger.[15,17] This change is clearly observed on comparison of the lower-energy band in the electronic spectra of bi- and tri-nuclear complexes (see Table 4 and Figure 4). In addition, the trinuclear complexes display a second band in the visible region at higher energy as observed[18] for the trinuclear angular complexes $[Rh_3\{\mu\text{-}PMe(CH_2PPh_2)_2\}_2(CO)_3X_2][BPh_4]$ (X = Cl, Br, or I). In conclusion, the conformation in Figure 2(*a*) is generally adopted by the trinuclear complexes herein described, whilst that in 2(*b*) is enforced if the metal fragment bonded to the S atoms, Rh(2), is too bulky to occupy the hole in the framework 2(*a*) which occurs in the compound $[RhPd_2(SC_5H_4N)_4(\eta^3\text{-}C_4H_7)_2][BF_4]$.[11]

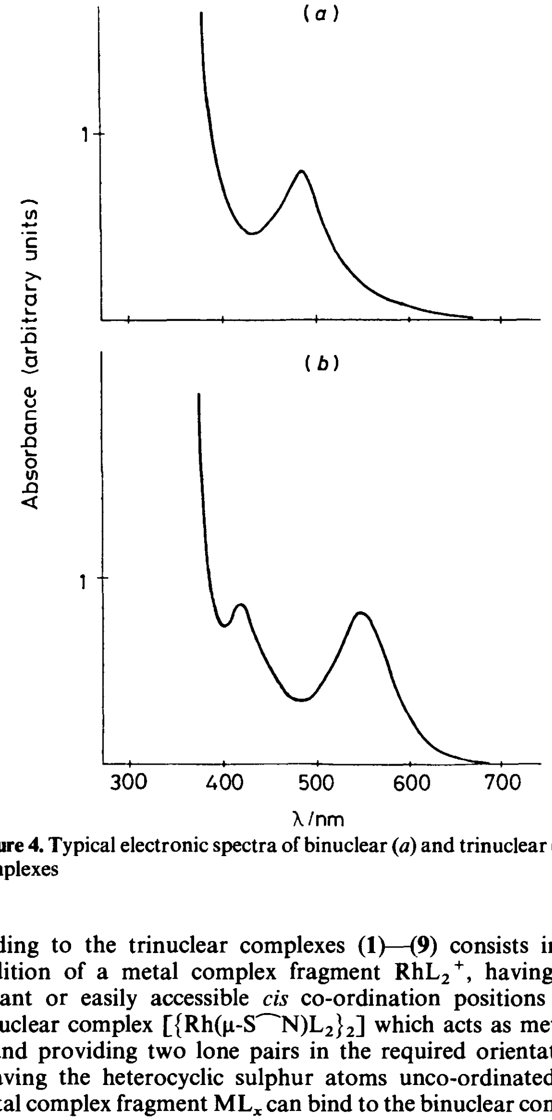

Figure 4. Typical electronic spectra of binuclear (*a*) and trinuclear (*b*) (**9**) complexes

Formation of the Trinuclear Complexes.—The synthetic route leading to the trinuclear complexes (**1**)—(**9**) consists in the addition of a metal complex fragment RhL_2^+, having two vacant or easily accessible *cis* co-ordination positions to a binuclear complex $[\{Rh(\mu\text{-}S^\frown N)L_2\}_2]$ which acts as metallo-ligand providing two lone pairs in the required orientations. Leaving the heterocyclic sulphur atoms unco-ordinated, the metal complex fragment ML_x can bind to the binuclear complex in two possible ways, as shown in the Scheme. We have shown[3] that in solution some of the parent binuclear complexes may undergo the change in the co-ordination mode of the bridging ligands described by $(a) \rightleftharpoons (b)$. Co-ordination of the metal complex fragment ML_x to structure (*b*) [equation (2)] would result in a trinuclear complex in which this fragment is at one of its ends. An inversion of the configuration of the bridging sulphur atom should occur and the complex will adopt the closed framework shown in Figure 2(*a*). On the other hand, the eight-membered ring '$Rh_2(\mu\text{-}N\text{–}C\text{–}S)_2$' in the structure (*a*) (Scheme) is extraordinarily flexible, allowing a facile interconversion of its three conformations $(c) \rightleftharpoons (a) \rightleftharpoons (d)$. Note the wide range of metal–metal distances allowed in the binuclear complexes. The entering metal complex fragment ML_x [equations (1) and (3)] then binds to the binuclear complexes through the sulphur atoms and remains at the vertex of the angle defined by the metal atoms.

Distinction between these two modes of formation is possible if either the metal or the ancillary ligands of the added species ML_x are different from those in the binuclear complex. Furthermore, addition of ML_x to binuclear complexes which do not undergo the transformation $(a) \rightleftharpoons (b)$ should give trinuclear complexes in a controlled way.

To test these hypotheses we have chosen the compounds $[\{Rh(\mu\text{-}C_7H_4NS_2)(CO)(PPh_3)\}_2]$ and $[\{Rh(\mu\text{-}C_7H_4NS_2)(tfbb)\}_2]^3$ as metallo-ligands. The latter exists in solution

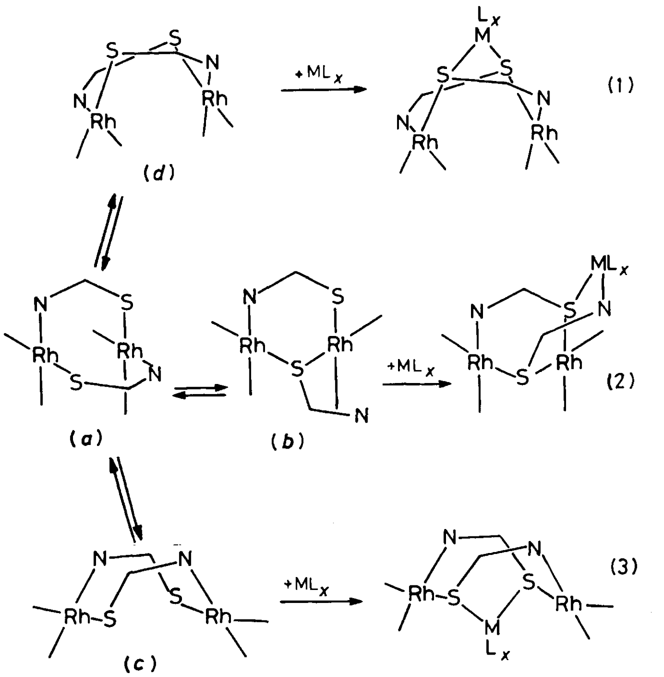

Scheme. Conformations of the '$Rh_2(\mu$-N–C–S$)_2$' ring and pathways of formation of the trinuclear complexes

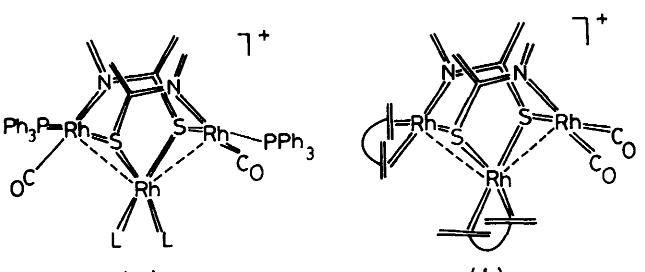

Figure 5. Structure of the complexes (**10**)—(**13**) (*a*) and (**14**) (*b*)

in at least two species due to the equilibrium (*a*) $\rightleftharpoons$ (*b*) (Scheme) whilst the former has structure (*a*). Both react with the appropriate species $[RhL_2(Me_2CO)_x]^+$ in acetone or alternatively with compounds $[\{Rh(\mu\text{-}Cl)L_2\}_2]$ in methanol to give deeply coloured solutions of the complexes $[Rh_3(\mu_3\text{-}C_7H_4NS_2)_2(CO)_2(PPh_3)_2L_2]^+$ [L_2 = cod, (**10**); nbd, (**11**); tfbb (**12**); or $(CO)_2$ (**13**)] and $[Rh_3(\mu_3\text{-}C_7H_4NS_2)_2(tfbb)_2L_2]^+$ ($L_2 = (CO)_2$, (**14**); or $(CO)(PPh_3)$, (**15**)] respectively, isolated as their perchlorate salts.

The synthesis of complexes (**10**)—(**13**) takes place cleanly giving a single isomer having the structure shown in Figure 5(*a*) as deduced from their spectroscopic properties (see Tables 1 and 3). Thus, they show equivalent phosphine and bridging ligands, the expected ν(CO) bands, and display two intense bands in the visible region (Table 4). Full confirmation of the structure of one of these complexes (**12**) has been carried out by single-crystal *X*-ray diffraction methods (see below). The formation of the single isomer shown in Figure 5(*a*) is a consequence of the mode of formation [equation (3), Scheme]. Significantly, no redistribution reactions of the trinuclear complexes (**10**)—(**13**) occur. The binuclear complex $[\{Rh(\mu\text{-}C_7H_4NS_2)(CO)(PPh_3)\}_2]$ behaves then like $[\{Pt(\mu\text{-}S)(PPh_3)_2\}_2]$[9] leading to aggregates of predetermined structure.

On the other hand a mixture of isomers of the trinuclear complexes derived from $[\{Rh(\mu\text{-}C_7H_4NS_2)(tfbb)\}_2]$ is expected. Nevertheless, complex (**14**) is isolated essentially as a single isomer having the structure shown in Figure 5(*b*), which can be purified by crystallization. Its spectroscopic properties (see Tables 1 and 3), *e.g.* the presence of the *cis*-$Rh(CO)_2$ moiety showing two ν(CO) bands and the inequivalence of the bridging ligands, are in accordance with the proposed structure. Complex (**14**) is then formed according to equation (2) (Scheme). In contrast, the synthesis of complex (**15**) is more complicated since a mixture of (**12**) and (**15**) [^{13}P-{^{1}H} n.m.r.: δ 42.5 p.p.m. d, ^1J(PRh) 166 Hz] results when the reaction is carried out at room or low temperature. Complex (**12**) results from a redistribution of the entering moiety '$Rh(CO)(PPh_3)$' and those already co-ordinated, 'Rh(tfbb),' in the binuclear complex, which contrasts with the stability of complexes (**10**)—(**14**). The rearrangement should be produced by reaction of the added species $[Rh(CO)(PPh_3)(Me_2CO)_x]^+$ with the already formed trinuclear complex (**15**). Effectively, addition of excess of $[Rh(CO)(PPh_3)(Me_2CO)_x]^+$ to a solution of $[Rh_3(\mu_3\text{-}SC_5H_4N)_2(tfbb)_3][ClO_4]$ in acetone renders a mixture of complexes in which complex (**12**) and $[\{Rh(\mu\text{-}C_7H_4NS_2)(CO)(PPh_3)\}_2]$ are detected by ^{31}P n.m.r. spectroscopy. We suggest that the attack of the electrophile $[Rh(CO)(PPh_3)(Me_2CO)_x]^+$ occurs at the bridging sulphur atom in the trinuclear complexes.

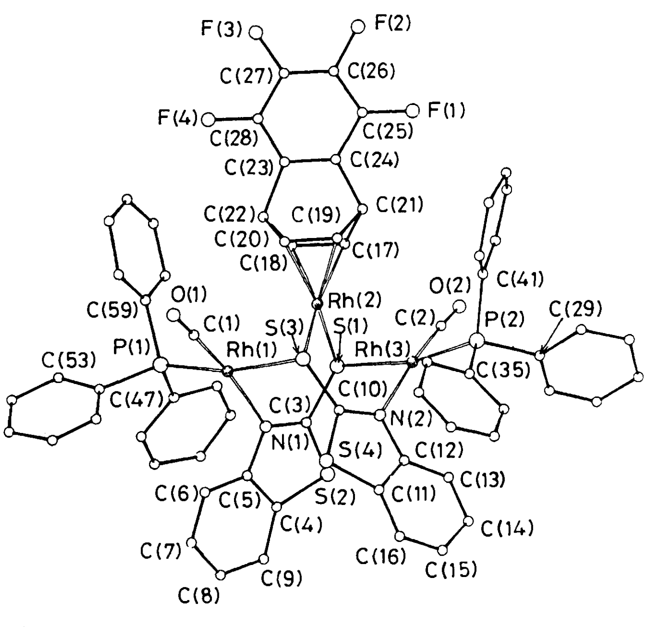

Figure 6. View of the cationic complex $[Rh_3(\mu_3\text{-}C_7H_4NS_2)_2(CO)_2(PPh_3)_2(tfbb)]^+$ (**12**) with the atomic numbering scheme

Description of the Crystal Structure of $[Rh_3(\mu_3\text{-}C_7H_4NS_2)_2(CO)_2(PPh_3)_2(tfbb)][ClO_4]$ (**12**).—The structure of complex (**12**) consists of $[Rh_3(\mu_3\text{-}C_7H_4NS_2)_2(CO)_2(PPh_3)_2(tfbb)]^+$ cations (Figure 6) and ClO_4^- anions. Selected bond distances and angles are listed in Table 5. The structure of this trinuclear cationic complex is very similar to that of (**4**) and can be derived from it by substituting the pyridine-2-thiolate ligands with the benzothiazole-2-thiolate ligands, triply bridging in the same manner, two carbonyl groups on the terminal Rh atoms with two PPh_3 ligands, and two carbonyl groups on the central Rh atom with a tfbb molecule interacting in a η^2 fashion through the two double bonds. If the midpoints of the C(17)–C(18) and C(19)–C(20) bonds, M(1) and M(2) respectively, are taken into account, the central Rh atom adopts a square-planar co-ordination [Rh(2)–M(1) 2.04(2) and Rh(2)–M(2) 2.00(2) Å]. The Rh(1)$\cdots$Rh(2) and Rh(2)$\cdots$Rh(3) separations are 3.033(3) and 2.994(4) Å with the Rh(1)–Rh(2)–Rh(3) angle of 112.0(1)°. The square-planar co-ordinations around the

Table 5. Selected bond distances (Å) and angles (°) in complex (**12**)*

Rh(1)···Rh(2)	3.033(3)	C(6)–C(7)	1.42(3)
Rh(2)···Rh(3)	2.994(4)	C(7)–C(8)	1.41(3)
Rh(1)–P(1)	2.269(7)	C(8)–C(9)	1.40(3)
Rh(1)–S(3)	2.386(6)	C(4)–C(9)	1.46(3)
Rh(1)–N(1)	2.150(17)	N(2)–C(10)	1.34(3)
Rh(1)–C(1)	1.80(3)	N(2)–C(12)	1.40(3)
Rh(2)–S(1)	2.383(6)	S(3)–C(10)	1.71(2)
Rh(2)–S(3)	2.374(6)	S(4)–C(10)	1.69(2)
Rh(2)–C(17)	2.14(2)	S(4)–C(11)	1.72(2)
Rh(2)–C(18)	2.18(2)	C(11)–C(12)	1.37(3)
Rh(2)–C(19)	2.11(2)	C(12)–C(13)	1.41(3)
Rh(2)–C(20)	2.14(2)	C(13)–C(14)	1.35(3)
Rh(3)–P(2)	2.284(7)	C(14)–C(15)	1.44(3)
Rh(3)–S(1)	2.411(6)	C(15)–C(16)	1.35(4)
Rh(3)–N(2)	2.136(16)	C(11)–C(16)	1.45(3)
Rh(3)–C(2)	1.80(2)	C(17)–C(18)	1.41(3)
N(1)–C(3)	1.32(3)	C(19)–C(20)	1.40(3)
N(1)–C(5)	1.43(2)	C(17)–C(21)	1.62(3)
S(1)–C(3)	1.76(2)	C(19)–C(21)	1.46(3)
S(2)–C(3)	1.66(2)	C(18)–C(22)	1.53(3)
S(2)–C(4)	1.75(2)	C(20)–C(22)	1.54(3)
C(4)–C(5)	1.37(3)	C(1)–O(1)	1.13(3)
C(5)–C(6)	1.38(3)	C(2)–O(2)	1.16(3)
P(1)–Rh(1)–N(1)	96.1(5)	Rh(2)–S(1)–C(3)	112.6(7)
N(1)–Rh(1)–S(3)	88.8(5)	Rh(3)–S(1)–C(3)	108.7(7)
S(3)–Rh(1)–C(1)	89.6(8)	C(3)–N(1)–Rh(1)	130.0(13)
C(1)–Rh(1)–P(1)	88.3(8)	C(5)–N(1)–Rh(1)	119.4(13)
S(1)–Rh(2)–S(3)	97.7(2)	C(10)–N(2)–Rh(3)	127.7(14)
M(1)–Rh(2)–M(2)	70.8(8)	C(12)–N(2)–Rh(3)	120.0(14)
S(1)–Rh(2)–M(1)	95.9(6)	N(1)–C(3)–S(1)	122.8(15)
S(3)–Rh(2)–M(2)	96.3(6)	N(1)–C(3)–S(2)	116.9(15)
P(2)–Rh(3)–N(2)	95.0(5)	S(1)–C(3)–S(2)	120.3(12)
N(2)–Rh(3)–S(1)	88.8(5)	C(3)–S(2)–C(4)	89.6(10)
S(1)–Rh(3)–C(2)	87.6(7)	N(2)–C(10)–S(3)	123.9(15)
C(2)–Rh(3)–P(2)	90.8(7)	N(2)–C(10)–S(4)	113.2(15)
Rh(1)–S(3)–Rh(2)	79.2(2)	S(3)–C(10)–S(4)	122.9(13)
Rh(1)–S(3)–C(10)	110.2(7)	C(10)–S(4)–C(11)	91.2(11)
Rh(2)–S(3)–C(10)	113.6(8)	Rh(1)–C(1)–O(1)	175(2)
Rh(2)–S(1)–Rh(3)	77.3(2)	Rh(3)–C(2)–O(2)	174(2)

* M(1) and M(2) are the midpoints of the C(17)–C(18) and C(19)–C(20) bonds.

terminal Rh atoms are more distorted than in (**4**) [deviations from the mean plane: through C(1), P(1), N(1), and S(3), C(1) 0.64(2), P(1) −0.036(6), N(1) 0.19(1), S(3) −0.031(6), and Rh(1) 0.236(3); through C(2), P(2), N(2), and S(1), C(2) 0.54(3), P(2) −0.029(6), N(2) 0.20(2), S(1) −0.027(6), and Rh(3) 0.223(3); and through S(1), S(3), M(1), and M(2), S(1) 0.008(5), S(3) −0.008(5), M(1) −0.20(2), M(2) 0.19(2), and Rh(2) 0.004(3) Å]. The co-ordination planes around Rh(1) and Rh(3) make a dihedral angle with that around Rh(2) of 73.7(3) and 72.5(3)° respectively. The Rh–S bonds [range 2.374(6)—2.411(6) Å] are comparable with those found in (**4**), whereas the Rh–N bonds are slightly longer [2.136(16) and 2.150(17) Å]. The benzothiazole-2-thiolate ligands are perfectly planar except for the atoms S(1) and S(3) which deviate from the mean planes through the benzothiazole moieties by 0.182(5) and 0.201(5) Å. The S···N bites of these ligands, 2.706(16) and 2.692(19) Å, are practically equal to those of the pyridine-2-thiolate ligands in (**4**).

The structure of (**12**) is comparable to that of the hetero-trinuclear complex $[Rh_2Ag(cod)_2(\mu_3\text{-}C_7H_4NS_2)_2(O_2ClO_2)]$ where the silver atom replaces the central Rh atom and the benzothiazole-2-thiolate ligands again triply bridge the three metals. The Rh–Ag–Rh chain is bent with an angle of 110.5(1)° very similar to that found in (**12**), even if the Rh···Ag distances, 2.796(3) Å, are much shorter than the Rh···Rh ones.[2]

In conclusion, ligands having a N–C–S donor moiety, such as pyridine-2-thiolate and benzothiazole-2-thiolate, are able to promote a large variety of co-ordination situations involving the nitrogen and sulphur atoms. Besides the usual modes[19,20] unidentate and chelate, we and others have shown that they can bridge two metal atoms either through the N and S atoms[1,3,21–24] or, more rarely, through the sulphur atom only.[3,25] In addition, we show here their almost unknown[26,27] ability to act as triple bridges and, particularly relevant, their use as backbones about which angular arrays of three metal atoms in close proximity can be constructed in a controlled way.

Experimental

The starting materials $[\{Rh(\mu\text{-}Cl)(diolefin)\}_2]$ (diolefin = cod, nbd, or tfbb), $[\{Rh(\mu\text{-}Cl)(CO)_2\}_2]$, $[\{Rh(\mu\text{-}SC_5H_4N)(diolefin)\}_2]$, $[\{Rh(\mu\text{-}C_7H_4NS_2)(diolefin)\}_2]$ (diolefin = cod, nbd, or tfbb), $[\{Rh(\mu\text{-}C_7H_4NS_2)(CO)(PPh_3)\}_2]$, and $[\{Rh(\mu\text{-}C_7H_4NS_2)(CO)_2\}_2]$[3] were prepared according to reported methods. All the reactions were carried out under a nitrogen atmosphere at room temperature using Schlenk techniques. Solvents were dried by standard methods and distilled under nitrogen immediately prior to use.

Proton and ^{31}P n.m.r. spectra were recorded on a Varian XL-200 spectrometer operating at 200.057 and 80.984 MHz respectively; chemical shifts are reported relative to tetramethylsilane and phosphoric acid as external references. I.r. spectra (range 4 000—200 cm^{-1}) were recorded on a Perkin-Elmer 783 spectrometer using Nujol mulls between polyethylene sheets or in solution in NaCl windows. Elemental analyses were carried out with a Perkin-Elmer 240B microanalyzer. Conductivities were measured in *ca.* 5×10^{-4} mol dm^{-3} acetone solutions using a Philips 9501/01 conductimeter. Visible–ultraviolet spectra were run on a Cary 17 spectrophotometer on acetone solutions of the complexes (range 700—330 nm).

Preparations of the Complexes.—$[Rh_3(\mu_3\text{-}SC_5H_4N)_2(diolefin)_3][ClO_4]$ (**1**)—(**3**). An acetone solution of $[Rh(diolefin)(Me_2CO)_x][ClO_4]$ (prepared by treating $[\{RhCl(diolefin)\}_2]$ (0.1 mmol) with $Ag[ClO_4]$ (41.47 mg, 0.2 mmol) in acetone (10 cm^3) for 30 min and filtering off the AgCl formed) was added slowly to a solution of the appropriate compound $[\{Rh(\mu\text{-}SC_5H_4N)(diolefin)\}_2]$ (0.2 mmol) in dichloromethane (5 cm^3). The deep green solutions were evaporated under vacuum to 1 cm^3. Slow addition of diethyl ether (5 cm^3) gave the compounds as microcrystalline solids which were filtered off, washed with diethyl ether, and vacuum-dried.

Complex (**4**). Carbon monoxide was bubbled through a solution of complexes (**1**)—(**3**) (0.2 mmol) in dichloromethane (5 cm^3) for 30 min. The deep violet solutions were evaporated under vacuum to 1 cm^3. Addition of diethyl ether (5 cm^3) under an atmosphere of carbon monoxide rendered the required compound as a crystalline solid which was filtered off, washed with diethyl ether, and dried under vacuum.

$[Rh_3(\mu_3\text{-}C_7H_4NS_2)_2(diolefin)_3][ClO_4]$ (**5**)—(**7**). A solution of $[Rh(diolefin)(Me_2CO)_x][ClO_4]$ (0.1 mmol) in acetone (10 cm^3) (prepared as described above) was added slowly to a solution of the appropriate compound $[Rh(\mu\text{-}C_7H_4NS_2)(diolefin)\}_2]$ (0.2 mmol) in dichloromethane (5 cm^3) to give deep green solutions of the complexes. Evaporation of the solutions under vacuum to 1 cm^3 and addition of diethyl ether (5 cm^3) gave the complexes as microcrystalline solids which were filtered off, washed with diethyl ether, and dried under vacuum.

Complex (**8**). *Method* (*a*). Carbon monoxide was bubbled through a dichloromethane solution (5 cm^3) of complex (**5**) (106 mg, 0.1 mmol) for 15 min giving a deep purple solution. Hexane (10 cm^3) was then added and the bubbling was continued for 30

Table 6. Fractional atomic co-ordinates (× 10^4) with estimated standard deviations (e.s.d.s) in parentheses for the non-hydrogen atoms of complex (**4**)

Atom	*X*/*a*	*Y*/*b*	*Z*/*c*
Rh(11)	1 778(1)	9 117(3)	474(1)
Rh(21)	1 030(1)	7 516(3)	61(1)
Rh(31)	541(1)	6 903(3)	1 110(1)
Cl(1)	327(2)	3 901(11)	3 531(3)
S(11)	1 499(1)	6 167(8)	801(2)
S(21)	824(1)	9 862(8)	784(2)
N(11)	1 564(4)	10 489(19)	1 265(6)
N(21)	1 016(4)	6 500(21)	1 760(7)
Rh(12)	4 423(1)	3 787(2)	7 897(1)
Rh(22)	3 591(1)	4 184(2)	7 538(1)
Rh(32)	3 157(1)	5 695(2)	8 566(1)
Cl(2)	2 299(2)	375(9)	3 875(3)
S(12)	3 885(1)	2 334(7)	8 376(2)
S(22)	3 702(1)	7 097(7)	8 095(2)
N(12)	4 420(4)	5 984(20)	8 557(6)
N(22)	3 534(4)	4 388(20)	9 251(6)
O(11)	1 952(4)	12 847(25)	−50(7)
O(21)	2 076(4)	7 214(22)	−656(7)
O(31)	588(5)	9 467(27)	−1 018(9)
O(41)	1 069(6)	3 975(33)	−731(10)
O(51)	186(5)	3 235(25)	1 424(7)
O(61)	−141(5)	7 524(28)	198(9)
O(71)	30(5)	3 417(25)	3 913(8)
O(81)	572(6)	5 220(30)	3 850(9)
O(91)	175(8)	4 734(41)	2 980(13)
O(101)	528(10)	2 480(56)	3 378(16)
C(11)	1 911(7)	11 401(37)	158(11)
C(21)	1 981(7)	7 970(35)	−207(11)
C(31)	747(7)	8 753(36)	−597(12)
C(41)	1 087(7)	5 373(39)	−446(12)
C(51)	333(7)	4 652(37)	1 309(11)
C(61)	137(7)	7 358(38)	560(12)
C(71)	1 187(7)	10 524(25)	1 378(8)
C(81)	1 062(5)	11 246(28)	1 954(9)
C(91)	1 353(6)	11 813(33)	2 403(10)
C(101)	1 738(6)	11 773(33)	2 270(10)
C(111)	1 843(6)	11 133(32)	1 708(13)
C(121)	1 388(5)	6 450(26)	1 601(8)
C(131)	1 704(6)	6 556(29)	2 055(9)
C(141)	1 630(6)	6 735(29)	2 701(9)
C(151)	1 247(6)	6 792(30)	2 865(9)
C(161)	937(5)	6 623(27)	2 376(9)
O(12)	5 038(5)	5 718(28)	7 234(8)
O(22)	4 412(5)	449(27)	7 017(8)
O(32)	3 330(5)	6 288(26)	6 353(8)
O(42)	3 307(5)	574(28)	6 938(9)
O(52)	2 468(5)	3 507(25)	8 935(8)
O(62)	2 634(6)	7 860(31)	7 703(9)
O(72)	2 425(5)	2 114(27)	3 593(8)
O(82)	2 357(5)	586(26)	4 529(9)
O(92)	2 493(7)	−1 094(36)	3 668(11)
O(102)	1 900(5)	165(24)	3 723(7)
C(12)	4 796(7)	4 945(35)	7 479(11)
C(22)	4 432(7)	1 818(36)	7 341(11)
C(32)	3 428(6)	5 544(32)	6 832(10)
C(42)	3 403(7)	1 975(39)	7 172(12)
C(52)	2 729(6)	4 374(32)	8 814(10)
C(62)	2 850(8)	7 032(38)	8 027(12)
C(72)	4 107(5)	7 001(25)	8 679(8)
C(82)	4 083(5)	8 155(28)	9 222(9)
C(92)	4 415(5)	8 107(28)	9 648(8)
C(102)	4 741(6)	7 184(32)	9 529(9)
C(112)	4 738(5)	6 099(28)	8 982(8)
C(122)	3 852(5)	3 380(24)	9 146(7)
C(132)	4 143(5)	2 919(26)	9 600(8)
C(142)	4 108(5)	3 509(29)	10 216(9)
C(152)	3 779(5)	4 655(26)	10 352(8)
C(162)	3 497(5)	4 973(27)	9 870(9)
Cl(3)	3 483(2)	−362(11)	678(3)
Cl(4)	2 985(2)	−111(12)	−465(4)
C(17)	3 017(8)	209(42)	371(13)

min to give a violet crystalline solid which was separated by filtration and washed with cold hexane (5 cm^3) and vacuum-dried. Yield: 45 mg, 52%.

Method (*b*). An acetone solution of $[Rh(CO)_2(Me_2CO)_x][ClO_4]$ (0.1 mmol) (prepared by treating $[\{Rh(\mu\text{-}Cl)(CO)_2\}_2]$ (19.34 mg, 0.05 mmol) with $Ag[ClO_4]$ (20.73 mg, 0.1 mmol) in acetone (10 cm^3) for 30 min and filtering off the AgCl formed) was added slowly to a solution of $[\{Rh(\mu\text{-}C_7H_4NS_2)(CO)_2\}_2]$ (65 mg, 0.1 mmol) in dichloromethane (5 cm^3). The solution was evaporated under vacuum to 1 cm^3. Addition of cold hexane rendered the complex which was filtered off, washed with cold hexane (5 cm^3), and dried under vacuum. Yield: 72 mg, 79%.

Complex (**9**). Carbon monoxide was bubbled through a solution of complex (**5**) (106 mg, 0.1 mmol) in dichloromethane (5 cm^3) for 15 min to give a solution of (**8**). Solid triphenylphosphine (79 mg, 0.3 mmol) was then added to give a dark red solution with evolution of carbon monoxide. The solvent was pumped off and the residue dissolved in methanol (1 cm^3). Addition of diethyl ether (20 cm^3) gave the complex as a crystalline solid which was filtered off, washed with diethyl ether, and vacuum-dried.

$[Rh_3(\mu_3\text{-}C_7H_4NS_2)_2(CO)_2(PPh_3)_2L_2][ClO_4]$ (**10**)—(**13**). *Method* (*a*). Solutions of the appropriate species $[RhL_2(Me_2CO)_x]ClO_4$ (0.1 mmol) [L_2 = cod, nbd, tfbb, or $(CO)_2$] in acetone (10 cm^3) (prepared as described above) were added *very slowly* to an orange solution of $[\{Rh(\mu\text{-}C_7H_4NS_2)(CO)(PPh_3)\}_2]$ (112 mg, 0.1 mmol) in dichloromethane (5 cm^3). The colour of the solutions turned deep green (L_2 = nbd or tfbb) or dark violet [L_2 = cod or $(CO)_2$]. Concentration of these solutions to *ca.* 1 cm^3 and slow addition of diethyl ether rendered the complexes as crystalline solids, which were filtered off, washed with diethyl ether, and then vacuum-dried.

Method (*b*). The appropriate solid complexes $[\{Rh(\mu\text{-}Cl)L_2\}_2]$ (0.05 mmol) [L_2 = cod, nbd, tfbb, or $(CO)_2$] were added to a solution of $[\{Rh(\mu\text{-}C_7H_4NS_2)(CO)(PPh_3)\}_2]$ (112 mg, 0.1 mmol) in methanol (10 cm^3). The colour of the solutions changed as above and then $Na[ClO_4]{\cdot}H_2O$ (14 mg, 0.1 mmol) in methanol (5 cm^3) was added. Complex (**12**) precipitates under these conditions and was isolated by filtration. For complexes (**10**), (**11**), and (**13**) the solvent was pumped off, the residue extracted with dichloromethane (15 cm^3) and then filtered. Concentration of the filtrate to *ca.* 1 cm^3 and addition of diethyl ether gave the complexes as crystals which were isolated by filtration.

Complex (**14**). A solution of $[Rh(CO)_2(Me_2CO)_x][ClO_4]$ (0.1 mmol) in acetone (10 cm^3) (prepared as described above) was added slowly to a solution of $[\{Rh(\mu\text{-}C_7H_4NS_2)(tfbb)\}_2]$ (96 mg, 0.1 mmol) in dichloromethane (5 cm^3). The deep green solution was evaporated under vacuum to 1 cm^3. Addition of diethyl ether rendered the complex which was filtered off, washed with diethyl ether, and dried under vacuum.

Crystal Structure Determinations of $[Rh_3(\mu_3\text{-}SC_5H_4N)_2(CO)_6][ClO_4]{\cdot}0.5CH_2Cl_2$ (**4**) *and* $[Rh_3(\mu_3\text{-}C_7H_4NS_2)_2(CO)_2$-

Table 7. Fractional atomic co-ordinates (× 10^4) with e.s.d.s in parentheses for the non-hydrogen atoms of complex (**12**)

Atom	*X*/*a*	*Y*/*b*	*Z*/*c*	Atom	*X*/*a*	*Y*/*b*	*Z*/*c*
Rh(1)	6 600(1)	1 126(2)	3 634(1)	C(22)	8 169(9)	887(21)	4 756(7)
Rh(2)	7 786(1)	2 627(2)	4 027(1)	C(23)	8 832(10)	829(22)	5 064(7)
Rh(3)	7 880(1)	5 225(2)	3 538(1)	C(24)	9 243(9)	1 774(21)	4 944(7)
Cl(1)	7 174(5)	670(13)	849(4)	C(25)	9 871(11)	1 880(24)	5 191(8)
S(1)	7 086(2)	4 465(6)	4 008(2)	C(26)	10 037(10)	1 005(24)	5 553(7)
S(2)	5 925(3)	5 483(6)	3 430(2)	C(27)	9 643(10)	96(25)	5 676(8)
S(3)	7 463(2)	1 851(6)	3 241(2)	C(28)	9 023(10)	−18(25)	5 439(8)
S(4)	6 803(3)	2 779(7)	2 304(2)	C(29)	9 006(9)	7 247(22)	3 085(7)
P(1)	5 962(3)	462(6)	4 171(2)	C(30)	9 649(11)	7 513(26)	2 998(8)
P(2)	8 766(3)	5 577(6)	3 180(2)	C(31)	9 834(10)	8 819(26)	2 944(8)
F(1)	10 268(6)	2 810(14)	5 072(4)	C(32)	9 386(12)	9 898(27)	2 950(9)
F(2)	10 622(5)	1 138(15)	5 805(4)	C(33)	8 753(10)	9 590(25)	3 027(8)
F(3)	9 813(6)	−775(16)	6 016(5)	C(34)	8 570(10)	8 345(24)	3 116(8)
F(4)	8 647(6)	−978(16)	5 545(5)	C(35)	8 666(9)	4 847(22)	2 565(7)
N(1)	6 166(7)	3 026(17)	3 496(5)	C(36)	8 627(10)	5 681(23)	2 176(8)
N(2)	7 346(7)	4 355(18)	2 925(6)	C(37)	8 494(11)	5 113(27)	1 721(9)
O(1)	7 070(8)	−1 569(20)	3 583(7)	C(38)	8 398(12)	3 724(29)	1 664(10)
O(2)	8 375(9)	6 868(21)	4 367(7)	C(39)	8 433(12)	2 960(27)	2 056(9)
O(3)	7 173(22)	1 908(54)	1 092(17)	C(40)	8 592(10)	3 492(25)	2 540(9)
O(4)	6 871(18)	−160(44)	1 104(14)	C(41)	9 494(10)	4 865(23)	3 490(8)
O(5)	7 682(22)	326(42)	731(15)	C(42)	9 728(11)	5 365(26)	3 939(8)
O(6)	6 736(17)	898(36)	426(13)	C(43)	10 310(12)	5 046(28)	4 193(9)
C(1)	6 891(11)	−536(27)	3 624(8)	C(44)	10 674(13)	4 171(30)	3 965(10)
C(2)	8 209(10)	6 176(26)	4 047(8)	C(45)	10 440(14)	3 540(31)	3 546(11)
C(3)	6 376(9)	4 208(21)	3 628(7)	C(46)	9 844(11)	3 936(26)	3 280(8)
C(4)	5 360(8)	4 389(20)	3 149(6)	C(47)	5 484(10)	1 893(23)	4 342(7)
C(5)	5 560(9)	3 110(22)	3 216(7)	C(48)	4 825(10)	1 803(23)	4 245(7)
C(6)	5 205(9)	2 056(21)	3 024(7)	C(49)	4 478(10)	2 928(23)	4 327(8)
C(7)	4 599(10)	2 343(24)	2 776(8)	C(50)	4 779(11)	4 124(25)	4 447(8)
C(8)	4 384(9)	3 654(22)	2 705(7)	C(51)	5 442(10)	4 153(23)	4 555(8)
C(9)	4 743(10)	4 730(24)	2 893(7)	C(52)	5 794(10)	3 028(24)	4 503(8)
C(10)	7 221(9)	3 075(21)	2 845(7)	C(53)	5 365(9)	−836(21)	4 001(7)
C(11)	6 813(10)	4 428(23)	2 160(8)	C(54)	5 068(10)	−1 400(23)	4 343(8)
C(12)	7 132(10)	5 138(24)	2 527(8)	C(55)	4 577(11)	−2 341(25)	4 193(8)
C(13)	7 195(10)	6 512(23)	2 478(8)	C(56)	4 435(10)	−2 677(24)	3 711(8)
C(14)	6 975(10)	7 121(23)	2 064(8)	C(57)	4 779(10)	−2 101(23)	3 388(8)
C(15)	6 675(10)	6 325(26)	1 679(8)	C(58)	5 240(10)	−1 225(25)	3 522(8)
C(16)	6 598(9)	5 009(23)	1 698(7)	C(59)	6 401(10)	−238(25)	4 701(8)
C(17)	8 343(9)	3 293(22)	4 668(7)	C(60)	6 595(11)	−1 542(27)	4 673(9)
C(18)	7 929(10)	2 302(24)	4 794(7)	C(61)	6 990(12)	−2 081(27)	5 091(9)
C(19)	8 712(9)	1 851(22)	4 131(7)	C(62)	7 137(12)	−1 282(30)	5 491(9)
C(20)	8 292(10)	855(23)	4 233(8)	C(63)	6 954(11)	−34(27)	5 521(9)
C(21)	8 996(9)	2 669(23)	4 529(7)	C(64)	6 576(11)	586(25)	5 126(8)

$(PPh_3)_2$(tfbb)][ClO_4] (**12**).—Prismatic crystals of approximate dimensions 0.15 × 0.19 × 0.25 (**4**) and 0.18 × 0.22 × 0.30 mm (**12**) were used.

Crystal data. (**4**), $C_{16}H_8ClN_2O_{10}Rh_3S_2\cdot0.5CH_2Cl_2$, $M = 839.00$, monoclinic, space group $P2_1/n$, $a = 34.460(11)$, $b = 7.027(3)$, $c = 21.109(8)$ Å, $\beta = 94.02(3)°$, $U = 5\,099(3)$ Å^3 (by least-squares refinement from the θ values of 25 accurately measured reflections, $\lambda = 0.710\,69$ Å), $Z = 8$, $D_c = 2.186$ g cm^{-3}, $F(000) = 3\,224$, $\mu(\text{Mo-}K_\alpha) = 23.12$ cm^{-1}.

(**12**), $C_{64}H_{44}ClF_4N_2O_6P_2Rh_3S_4$, $M = 1\,547.41$, monoclinic, space group $P2_1/c$, $a = 21.299(8)$, $b = 10.139(6)$, $c = 28.293(11)$ Å, $\beta = 97.53(2)°$, $U = 6\,057(5)$ Å^3 (by least-squares refinement from the θ values of 27 accurately measured reflections, $\lambda = 0.710\,69$ Å), $Z = 4$, $D_c = 1.697$ g cm^{-3}, $F(000) = 3\,088$, $\mu(\text{Mo-}K_\alpha) = 10.89$ cm^{-1}.

Data collection and processing. A Siemens AED single-crystal diffractometer (θ—2θ scan mode, niobium-filtered Mo-K_α radiation) was employed. All reflections with θ in the ranges 3—24° (**4**) and 3—23° (**12**) were measured; of 7 954 (**4**) and 8 467 (**12**) independent reflections, 3 412 (**4**) and 2 854 (**12**), having $I > 2\sigma(I)$, were considered observed and used in the analyses. No absorption correction was applied.

Structure solutions and refinements. Direct and Fourier methods, full-matrix least-squares refinements with anisotropic thermal parameters in the last cycles for the Rh, S, Cl (of the perchlorate anion), and N atoms (**4**) and for Rh, S, Cl, P, F, and O (of the carbonyl ligands) (**12**). All the hydrogen atoms of complexes (**4**) and of (**12**) were placed at their calculated positions (C–H 1.08 Å) and introduced in the final structure-factor calculations. For both structures a weighting scheme $w = K[\sigma^2(F_o) + gF_o^2]^{-1}$ was used in the last cycles of refinement with $K = 0.668$ (**4**) and 0.567 (**12**) and $g = 0.0050$ (**4**) and 0.0052 (**12**). Final R and R' values were 0.0572 and 0.0745 (**4**) and 0.0548 and 0.0664 (**12**) respectively. The SHELX system of computer programs was used.[28] Atomic scattering factors, corrected for anomalous dispersion, were taken from ref. 29. Final atomic co-ordinates for the non-hydrogen atoms are given in Tables 6 (**4**) and 7 (**12**) respectively. All calculations were carried out on the CRAY X-MP/12 computer of the Centro di Calcolo Elettronico Interuniversitario dell'Italia Nord-Orientale, Bologna and on the GOULD POWERNODE 6040 of the Centro di Studio per la Strutturistica Diffrattometrica del C.N.R., Parma.

Additional material available from the Cambridge Crystallographic Data Centre comprises H-atom co-ordinates, thermal parameters, and remaining bond distances and angles.

Acknowledgements

We thank the Comisión Asesora de Investigación Cientifica y Técnica, Consejo Superior de Investigaciones Cientificas-Consiglio Nationale della Ricerca. Joint Programme for financial support and Diputación General de Aragón for a grant (to J. J. P-T.).

References

1 L. A. Oro, M. A. Ciriano, F. Viguri, A. Tiripicchio, M. Tiripicchio-Camellini, and F. J. Lahoz, Proceedings of the XII International Conference on Organometallic Chemistry, Vienna, 1985, p. 410; *Nouv. J. Chim.*, 1986, **10**, 75.

2 M. A. Ciriano, L. A. Oro, J. J. Pérez-Torrente, A. Tiripicchio, and M. Tiripicchio-Camellini, *J. Chem. Soc., Chem. Commun.*, 1986, 1737.

3 M. A. Ciriano, F. Viguri, J. J. Pérez-Torrente, F. J. Lahoz, L. A. Oro, A. Tiripicchio, and M. Tiripicchio-Camellini, *J. Chem. Soc., Dalton Trans.*, 1989, 25.

4 M. A. Ciriano, F. Viguri, L. A. Oro, A. Tiripicchio, and M. Tiripicchio-Camellini, *Angew. Chem.*, 1987, **99**, 452; *Angew. Chem., Int. Ed. Engl.*, 1987, **26**, 444.

5 M. A. Ciriano, S. Sebastián. L. A. Oro, A. Tiripicchio, M. Tiripicchio-Camellini, and F. J. Lahoz, *Angew. Chem.*, 1988, **100**, 406; *Angew. Chem., Int. Ed. Engl.*, 1988, **27**, 402.

6 L. A. Oro, M. A. Ciriano, B. E. Villarroya, A. Tiripicchio, and F. J. Lahoz, *J. Chem. Soc., Dalton Trans.*, 1985, 1891.

7 (*a*) A. M. Manotti-Lanfredi, A. Tiripicchio, R. Usón, L. A. Oro, M. A. Ciriano, and B. E. Villarroya, *Inorg. Chim. Acta*, 1984, **88**, L9; (*b*) M. A. Ciriano, B. E. Villarroya, and L. A. Oro, *ibid.*, 1986, **120**, 43 and refs. therein.

8 M. A. Ciriano, B. E. Villarroya, L. A. Oro, M. C. Apreda, C. Foces-Foces, and F. H. Cano, *J. Organomet. Chem.*, 1989, **366**, 377.

9 D. I. Gilmour, M. A. Luke, and D. M. P. Mingos, *J. Chem. Soc., Dalton Trans.*, 1987, 335.

10 M. Cowie and T. Sielich, *J. Organomet. Chem.*, 1988, **348**, 241.

11 A. J. Deeming, M. N. Meah, P. A. Bates, and M. B. Hursthouse, *J. Chem. Soc., Dalton Trans.*, 1988, 235.

12 A. L. Balch and B. Tulyathan, *Inorg. Chem.*, 1977, **16**, 2840.

13 W. A. Fordyce and G. A. Crosby, *J. Am. Chem. Soc.*, 1982, **104**, 985.

14 G. S. Rodman and K. R. Mann, *Inorg. Chem.*, 1985, **24**, 3507.

15 K. R. Mann, N. S. Lewis, R. M. Williams, H. B. Gray, and J. G. Gordon, II, *Inorg. Chem.*, 1978, **17**, 828.

16 S. F. Rice, V. M. Miskowski, and H. B. Gray, *Inorg. Chem.*, 1988, **27**, 4704.

17 A. L. Balch, L. A. Fossett, J. K. Nagle, and M. M. Olmstead, *J. Am. Chem. Soc.*, 1988, **110**, 6732.

18 A. L. Balch, L. A. Fosset, R. R. Guimerans, M. M. Olmstead, P. E. Reedy, jun., and F. E. Wood, *Inorg. Chem.*, 1986, **25**, 1248.

19 E. S. Raper, *Coord. Chem. Rev.*, 1985, **61**, 115.

20 P. Mura, B. G. Olby, P. A. Bates, and M. B. Hursthouse, *J. Chem. Soc., Dalton Trans.*, 1985, 201 and refs. therein.

21 A. J. Deeming, M. N. Meah, H. M. Dawes, and M. B. Hursthouse, *J. Organomet. Chem.*, 1986, **299**, C25.

22 K. Umakoshi, I. Kinosita, and S. Ooi, *Inorg. Chim. Acta*, 1987, **127**, L41.

23 D. M. L. Goodgame, R. W. Rollins, A. M. Z. Slawin, D. J. Williams, and P. W. Zard, *Inorg. Chim. Acta*, 1986, **120**, 91.

24 M. Cowie and T. Sielisch, *Organometallics*, 1988, **7**, 707.

25 G. Le Borgne and D. Grandjean, *J. Organomet. Chem.*, 1975, **92**, 381.

26 S. Jeanin, Y. Jeanin, and G. Lavigne, *Inorg. Chem.*, 1978, **17**, 2103.

27 A. J. Deeming, M. N. Meah, P. Bates, and M. Hursthouse, *J. Chem. Soc., Dalton Trans.*, 1988, 2193.

28 G. M. Sheldrick, SHELX Program for crystal structure determination, University of Cambridge, 1976.

29 'International Tables for *X*-Ray Crystallography,' Kynoch Press, Birmingham, 1974, vol. 4.

Received 1st *August* 1989; *Paper* 9/03256H